Goal functional evaluations for Poisson's problem and phase-field fracture using PU-based DWR mesh adaptivity

Bernhard Endtmayer and Thomas Wick*

JKU & RICAM Linz
* (soon: École Polytechnique, Palaiseau, France)

Jul 5, 2016
AANMPDE(JS)-9-16 in Strobl, Austria

Overview

1. Motivation
2. Phase-field fracture in elasticity
3. Goal functional evaluations with the PU-DWR method
4. Towards multiple goal functionals evaluations (contributed by a young Junior Scientist)
5. Conclusions

The PDE system of variational/phase-field fracture[1]

Formulation

Define $V := H_0^1(B), W_{in} := \{w \in H^1(B) | \, w \leq \varphi^{old} \leq 1 \text{ a.e. on } B\}$, *and* $W := H^1(B)$. *For the loading steps* $n = 1, 2, 3, \ldots$: *Find vector-valued displacements and a scalar-valued phase-field variable* $(u, \varphi) \in \{u_D + V\} \times W$ *such that*

$$\Big(\big((1-\kappa)\varphi^2 + \kappa\big)\, \sigma(u), e(w) \Big) = 0 \quad \forall w \in V, \tag{1}$$

and

$$\begin{aligned} &(1-\kappa)(\varphi\, \sigma(u) : e(u), \psi - \varphi) \\ &+ G_c \Big(-\frac{1}{\varepsilon}(1-\varphi, \psi - \varphi) + \varepsilon(\nabla\varphi, \nabla(\psi - \varphi)) \Big) \geq 0 \quad \psi \in W_{in} \cap L^\infty(B) \end{aligned} \tag{2}$$

Therein, $\varepsilon, \kappa > 0$ *and* $\kappa = o(\varepsilon)$, *and* G_c *is the critical energy release rate. Moreover,*

$$\sigma := \sigma(u) = 2\mu e(u) + \lambda \, tr(e(u)) I.$$

Here, μ *and* λ *are material parameters,* $e(u) = \frac{1}{2}(\nabla u + \nabla u^T)$ *is the strain tensor, and* I *the identity matrix. Key challenges are:*

- *Relation of* ε *to spatial discretization parameter* h;
- *Non-convexity of the related energy functional due to* $\Big(\big((1-\kappa)\varphi^2 + \kappa\big)\, \sigma(u), e(w) \Big)$.

[1] Francfort/Marigo; 1998, Bourdin et al.; 2000, Miehe et al.; 2010

A first example: damage and fatigue of screws

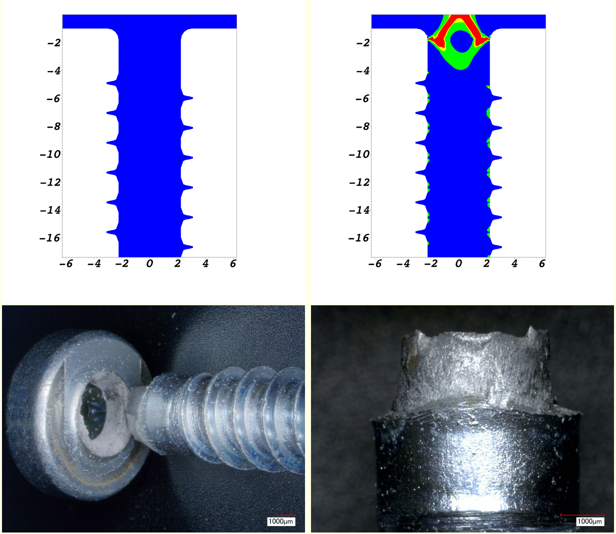

Figure: Industrial collaboration: Uniaxial tension and crack nucleation at points with highest stresses. Experimental data from D. Wick (EJOT, Germany).

A first example: damage and fatigue of screws

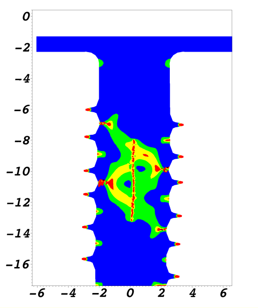

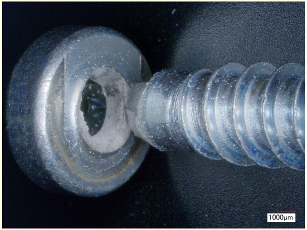

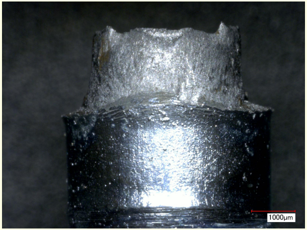

Figure: Industrial collaboration: Uniaxial tension and crack nucleation at points with highest stresses. Experimental data from D. Wick (EJOT, Germany).

A 2nd example: Two perpendicular fractures in a 3D heterogeneous porous medium [2]

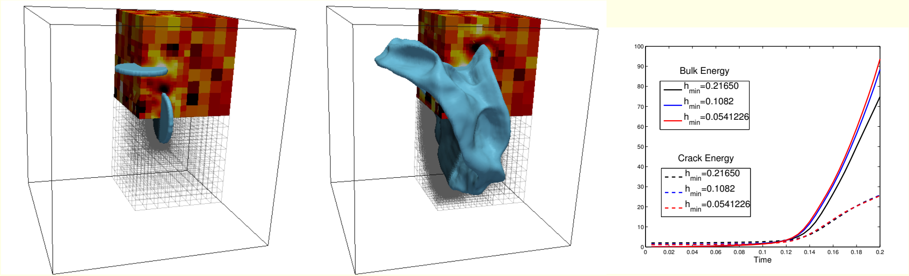

Figure: Two of snapshots of fractures propagating at each time step number n in three dimensional heterogeneous media. Both fractures grow non-planarly, then they join at $n = 11$ and start branching at $n = 13$. At right, mesh refinement studies show computational stability for energy computations.

[2] Lee/Wheeler/Wick; CMAME, 2016

Philosophy of our analysis and discretization

- Formulation as a semi-linear form:

Formulation

Find $U := \{u, \varphi\} \in V \times W$ *such that*

$$A(U)(\Psi - U) \geq 0 \quad \forall \Psi := \{w, \psi\} \in V \times W_{in}. \tag{3}$$

- Relaxing the inequality constraint $\partial_t \varphi \leq 0$ (e.g., augmented Lagrangian);
- Discretization in time (incremental formulation);
- Adaptive discretization in space;
- Newton's method (needs to be modified for fully monolithic solution!)

A monolithically-coupled formulation

Formulation

Given $\varphi^{n-1}, \tilde{\varphi} \in H^1(B)$. *For the loading steps* $n = 1, 2, 3, \ldots$*: Find* $U^n := U = \{u, \varphi\} \in \{u_D + V\} \times W$ *such that*

$$\begin{aligned} A(U)(\Psi) = & \Big(\big((1-\kappa)\tilde{\varphi}^2 + \kappa\big)\, \sigma(u), e(w) \Big) \\ & + (1-\kappa)(\varphi\, \sigma(u) : e(u), \psi) + G_c \Big(-\frac{1}{\varepsilon}(1-\varphi, \psi) + \varepsilon(\nabla\varphi, \nabla\psi) \Big) \\ & + ([\Xi + \gamma(\varphi - \varphi^{n-1})]^+, \psi) \\ = & \; 0 \quad \forall \Psi := \{w, \psi\} \in V \times W, \end{aligned}$$

where $\tilde{\varphi}$ *is a linear extrapolation of* φ^{n-1} *and* φ^{n-2}.

A monolithically-coupled formulation

Formulation

Given $\varphi^{n-1}, \tilde{\varphi} \in H^1(B)$. For the loading steps $n = 1, 2, 3, \ldots$: Find $U^n := U = \{u, \varphi\} \in \{u_D + V\} \times W$ such that

$$
\begin{aligned}
A(U)(\Psi) = \Big(\big((1-\kappa)\tilde{\varphi}^2 + \kappa\big)\, \sigma(u), e(w) \Big) \\
+ (1-\kappa)(\varphi\, \sigma(u) : e(u), \psi) + G_c\Big(-\frac{1}{\varepsilon}(1-\varphi, \psi) + \varepsilon(\nabla\varphi, \nabla\psi) \Big) \\
+ ([\Xi + \gamma(\varphi - \varphi^{n-1})]^+, \psi) \\
= 0 \quad \forall \Psi := \{w, \psi\} \in V \times W,
\end{aligned}
$$

where $\tilde{\varphi}$ is a linear extrapolation of φ^{n-1} and φ^{n-2}.

Why monolithic?

1. High accuracy of coupling conditions;
2. Numerical stability and implicit discretizations (e.g., in FSI - added-mass effect);
3. Consistent modeling of gradient-based optimization and dual-weighted error estimation;
4. Space-time formulations;
5. Finally, sometimes, the monolithic solution is even more efficient than subiterations (Gerasimov/Lorenzis; 2016, CMAME).

Adaptive discretization in space [3]

- Adaptive spatial discretization:
  - Galerkin finite element scheme with H^1 conforming discrete spaces $V_h \subset V$ and $W_h \subset W$ consisting of bilinear functions Q_1^c on quadrilaterals/hexahedra.
  - The key challenge is the relation of the model regularization parameter ε and the spatial mesh size h (high mesh resolution required!) since $h < \varepsilon$.

→ Predictor-corrector mesh adaptivity with hanging nodes (the mesh grows with the fracture).

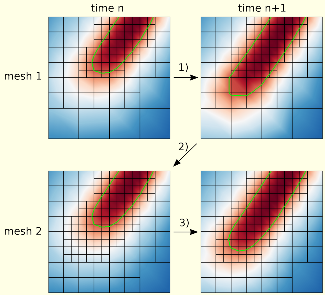

Figure: Predictor-corrector scheme: 1. advance in time, crack leaves fine mesh. 2. refine and go back in time (interpolate old solution). 3. advance in time on new mesh. Repeat until mesh doesn't change anymore. Refinement is triggered for $\varphi < C = 0.2$ (green contour line) here.

[3] Heister/Wheeler/Wick; CMAME, 2015

Basic structure of Newton's method

Formulation

Find $U_h \in \{u_D^h + V_h\} \times W_h$ *such that*

$$A(U_h)(\Psi) = 0 \quad \forall \Psi := \{w, \psi\} \in V_h \times W_h. \tag{4}$$

To solve this nonlinear problem, we employ an error-oriented Newton[4] *scheme within an inexact augmented Lagrangian loop.*

Formulation (Newton as defect-correction scheme)

For the iteration steps $m = 0, 1, 2, \ldots$, *the Newton update* $\delta U_h := \{\delta u_h, \delta \varphi_h\} \in V_h \times W_h$ *is computed by solving:*

$$\begin{aligned} A'(U_{h,m})(\delta U_h, \psi) &= -A(U_{h,m})(\Psi) \quad \forall \Psi \in V_h \times W_h, \\ U_{h,m+1} &= U_{h,m} + \omega \delta U_h, \end{aligned} \tag{5}$$

with a line search parameter $\omega \in (0, 1]$.

[4] P. Deuflhard; Newton Methods for Nonlinear Problems, 2011

Numerical tests[5]

- Single edge notched shear test.

[5] Implementation in open-source FE package deal.II (C++)

Single edge notched shear test in mechanics [6] [7]

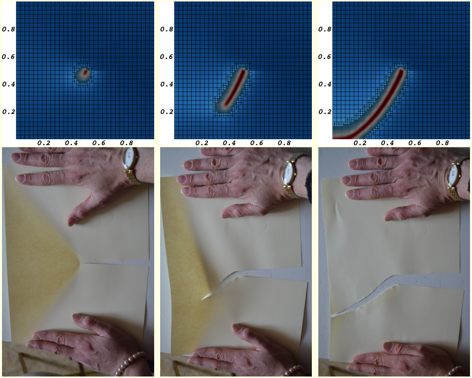

Figure: Comparison of experiment and numerical simulation.

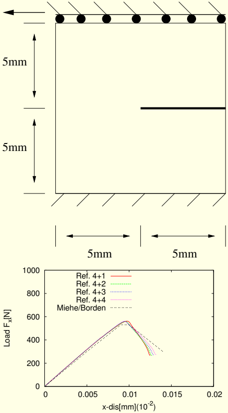

Figure: Setting and functional evaluation in terms of the load-displacement curve

---

[6] All parameters taken from Miehe et al. (2010) CMAME

[7] In addition, stress is split into tensile and compressive parts - again Miehe et al. 2010 / Amor et al. 2009

Goals

- Computational analysis of Γ-convergence properties, i.e., interplay of ε and h:
  - Case 1: $\varepsilon = 2h$,
  - Case 2: $\varepsilon = ch^{0.5}, c = 0.25$,
  - Case 3: $\varepsilon = ch^{0.25}, c = 0.125$.

Goals

- Computational analysis of Γ-convergence properties, i.e., interplay of ε and h:
  - Case 1: $\varepsilon = 2h$,
  - Case 2: $\varepsilon = ch^{0.5}, c = 0.25$,
  - Case 3: $\varepsilon = ch^{0.25}, c = 0.125$.
- Wall clock comparisons to show effectiveness of predictor-corrector mesh refinement.
- Complete numerical analysis not yet present in the literature!

Results: Crack path

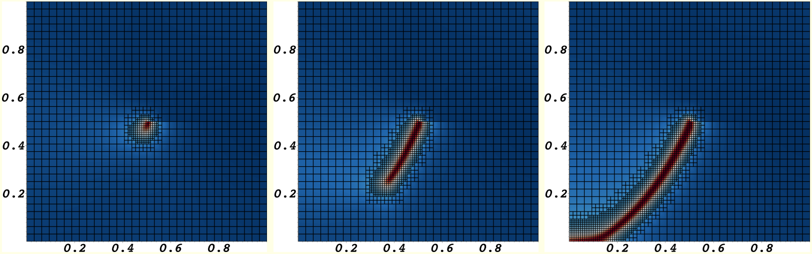

Figure: Crack path on $4 + 2$-refined meshes. Crack propagation in red and dynamic mesh refinement at different times $T = 100, 120, 150$ using predictor-corrector refinement with $C = 0.8$.

Results: Spatial refinement for different ε

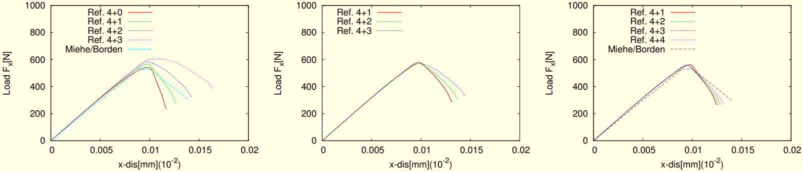

Figure: Mesh refinement studies for the three different Cases 1,2,3. We observe that if we choose h and ε according to the theoretical requirement of Γ convergence with $h = o(\varepsilon)$, then spatial mesh convergence is obtained (Cases 2+3)

Results: Wall clock time and computational cost

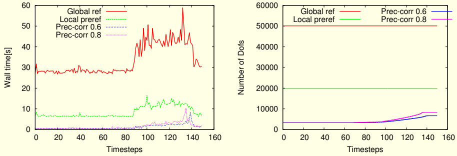

Figure: Comparison of computational cost in terms of the wall clock time (left) and corresponding evolution of the degrees of freedom. The wall clock time is measured for each time step.

Table: Comparison of computational cost for different refinement strategies.

	Time/s	Number of steps	DoFs: min/avg/max
global refinement	5036	151	50115
local prerefinement	1277	151	19746
predictor/corrector (0.8)	233	151+63	3315/4731/8286
predictor/corrector (0.6)	184	151+53	3315/4225/6666

Remarks to error estimation for phase-field fracture

- Define a goal functional $J(u)$:

$$J(u) = u(x_0, y_0), \quad \text{or} \quad J(\varphi) = \int_\Gamma \varphi \, ds,$$

or a global norm.

- In phase-field fracture, the error must be split into a model error and a discretization error

$$J(U) - J(U_h) = J(U) - J(U_\varepsilon) + J(U_\varepsilon) - J(U_{\varepsilon,h}),$$

thus

$$|J(U) - J(U_h)| \leq \underbrace{|J(U) - J(U_\varepsilon)|}_{\text{Model err.}} + \underbrace{|J(U_\varepsilon) - J(U_{\varepsilon,h})|}_{\text{Discretization err.}}.$$

Observation: Poisson's problem on slit domain [8]

- Set $\varepsilon = ch^l$ with
  - Case 1: $c = 2.0, l = 1$,
  - Case 2: $c = 0.5, l = 0.5$,
  - Case 3: $c = 0.5, l = 0.25$.

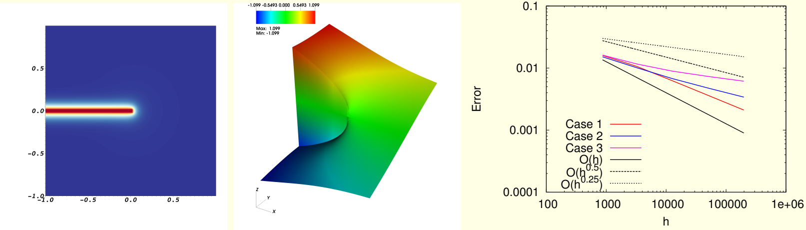

Figure: Crack, denoted in red color, (top) and 3D plot of the displacement field to show the discontinuity along the line $(x, 0)$ for $-1 \leq x \leq 0$ and comparison of convergence rates for a point value evaluation. Manufactured solution for $\varepsilon = 0$ (true slit domain) by Andersson/Mikayelyan; arXiv, 2015.

[8] T. Wick; Comp. Mech, 2016

PU-DWR for goal functional evaluations

- Use a posteriori error estimation for accurate measurements of quantities of interest (i.e., goal functionals):

$$|J(U) - J(U_h)| \approx \eta.$$

- Error representation is weighted by local adjoint sensitivity measures $Z \in X$ (exactly the same as for gradient-based optimization)

⇒ Solve a dual problem to obtain these sensitivity measures

- To localize the error estimator to obtain indicators for refinement, the influence of neighboring elements is required [9].
- Here, we keep the weak form [10] (in contrast to the classical method) and add a partition-of-unity (PU)

⇒ This PU-DWR is (very) easy to implement and to analyze!

- Use local error indicators η_i to mark cells for refinement (or possibly for coarsening)
- The algorithm follows the standard procedure for mesh adaptivity:

Solve, Estimate, Mark, Adapt

[9] Carstensen/Verfürth; SINUM, 1999
[10] Similar to Braack/Ern; 2003

PU-DWR for goal functional evaluations [11]

Proposition (Wick 2016)

For the finite element approximation of the phase-field problem, we have the a posteriori error estimate:

$$
\begin{aligned}
|J(U) - J(U_h)| \le \sum_i^N |\eta_i| = \sum_i^N \Big| \Big(-((1-\kappa)\tilde{\varphi}_h^2 - \kappa)\, \sigma^+(u_h), e(w_h) \Big) \\
- (\sigma^-(u_h), e(w_h)) - (\tilde{\varphi}^2 p, \nabla \cdot w_h) \\
- (1-\kappa)(\varphi_h\, \sigma^+(u_h) : e(u_h), \psi_h) - 2(\varphi_h\, p\, \nabla \cdot u_h, \psi_h) \\
- G_c \Big(-\frac{1}{\varepsilon}(1-\varphi_h, \psi_h) + \varepsilon(\nabla \varphi_h, \nabla \psi_h) \Big) - (\gamma[\varphi - \varphi^{n-1}]^+, \psi) \Big|,
\end{aligned}
$$

where the weighting functions are defined as

$$
w := (w_{2h}^{(2)} - z_h^u)\chi_h^i, \qquad \psi := (\psi_{2h}^{(2)} - z_h^\varphi)\chi_h^i.
$$

The first factors $w_{2h}^{(2)} - z_h^u$ and $\psi_{2h}^{(2)} - z_h^\varphi$ of the weights are standard. Here, $w_{2h}^{(2)}$ is a higher-order finite element approximation (i.e., Q_2^c) of the dual solution z^u, respectively for $\psi_{2h}^{(2)}$ and z^φ. The second function χ_h^i is a partition-of-unity.

[11] Richter/Wick; 2015, CAM

PU-DWR for goal functional evaluations (cont'd)

Proof.

- We know the general error representation for the primal estimator[12]:

$$
\begin{aligned}
J(U) - J(U_h) = B(Z - i_h Z) - A(U_h)(Z - i_h Z) \\
+ R^2(U - U_h, Z - Z_h),
\end{aligned}
$$

  where i_h denotes an interpolation operator from the continuous spaces into the FE spaces.

- The functional and semilinear forms are defined as

$$
\begin{aligned}
& B(Z - i_h Z) = -(\tilde{\varphi}^2 p, \operatorname{div}(z^u - i_h z^u)), \\
& A(U_h)(Z - i_h Z) \\
& \quad = \Big(\big((1-\kappa)\tilde{\varphi}^2 + \kappa\big)\, \sigma^+(u), e(z^u - i_h z^u) \Big) \\
& \qquad + (\sigma^-(u), e(z^u - i_h z^u)) \\
& \qquad + (1-\kappa)(\varphi\, \sigma^+(u) : e(u), z^\varphi - i_h z^\varphi) \\
& \qquad + 2(\varphi\, p \operatorname{div} u, z^\varphi - i_h z^\varphi) \\
& \qquad + G_c \Big(-\frac{1}{\varepsilon}(1-\varphi, \psi) + \varepsilon(\nabla\varphi, \nabla(z^\varphi - i_h z^\varphi)) \Big) \\
& \qquad + (\gamma[\varphi - \varphi^{n-1}]^+, z^\varphi - i_h z^\varphi).
\end{aligned}
$$

[12] Becker/Rannacher; 2001, Acta Numerica

PU-DWR for goal functional evaluations (cont'd)

- Taking the absolute value yields:

$$|J(U) - J(U_h)| \le |B(Z - i_h Z) - A(U_h)(Z - i_h Z)| \\ + |R^2(U - U_h, Z - Z_h)|.$$

Neglecting the remainder term and introducing the PU χ_h^i and summing over all degrees of freedom $i = 1, \dots, N$ brings us to:

$$|J(U) - J(U_h)| \\ \le \sum_i^N |B((Z - i_h Z)\chi_h^i) - A(U_h)((Z - i_h Z)\chi_h^i)|.$$

Inserting the definitions of $B(Z - i_h Z)$ and $A(U_h)(Z - i_h Z)$ and using the short notation $w := (w_{2h}^{(2)} - z_h^u)\chi_h^i$ and $\psi := (\psi_{2h}^{(2)} - z_h^\varphi)\chi_h^i$ yields the statement. Q.E.D.

Numerical results

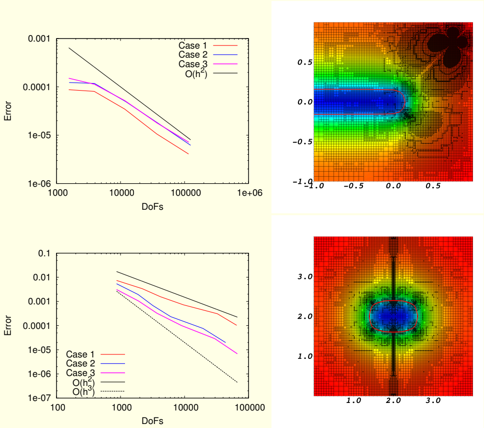

Figure: Top: point functional evaluation in the slit domain (but the slit is not given in the geometry but through phase-field). Bottom: Sneddon's test (elasticity with a given pressure p) and computation of $\int_\Gamma \varphi \, ds$ as goal functional. In both computations the crack tip is also refined - as expected.

Multiple goal functional evaluations [14]

- We are given N goal functionals $J_i, i = 1, \ldots, N$;
- Why? Specifically in flow and multiphysics problems such as Navier-Stokes flow, porous media, phase-field fracture, fluid-structure interaction, etc. the purpose might be on several quantities of interest;
- Challenge: In a naive and standard approach, we need to solve N dual problems: Find Z_i such that $A(U, Z_i) = J_i(U)$ for all $U \in V$.
- We follow Hartmann/Houston (2003) and Hartmann (2008) and use an approach in which only 2 additional problems need to be solved;
- At the same time we employ again a PU-localization for the error estimator;
- Current state[13]: Poisson's problem on l-shaped domains; next step: slit domain, which then already be compared to the phase-field results.

[13] Endtmayer/Wick; Ongoing work, 2016

[14] Hartmann/Houston; 2003, Hartmann; SISC, 2008

Combined functional

Idea:

- combine the functionals to a new functional $J_c(.)$, where

$$J_c(v) := \sum_i^N w_i J_i(v)$$

  for some weights w_i (not only positive ones)

- the choice of these weights is very crucial
- bad choice of weights maybe leads to error cancelling.

Algorithm

1. Compute the approximate solution $A(U_h, \Psi_h) = F(\Psi_h)$
2. Solve a discrete error problem (or also called dual-dual) $A(E, \Psi) = R_{U_h}(\Psi)$ (this dual-dual problem is only needed for the signs of the weights w_i!!)
3. Construct the combined functional $J_c(\Psi)$
4. If $|J_c(U) - J_c(U_h)| = |J_c(E)| < TOL$ stop
5. Else: Solve the dual problem $A(U, Z) = J_c(U)$ for the weights of the error functional
6. Compute local error estimators $|\eta_i|$
7. If $|\eta_i| < \frac{1}{n_h} \sum_i |\eta_i|$ we flag i-th element for refinement
8. Refine all the flagged elements in the mesh
9. Go to 1

Numerical results

First of all we consider the problem (L-shaped domain):

$$\Omega = (-1,1) \times (-1,1) \backslash (-1,0) \times (-1,0)$$
$$-\Delta u(x,y) = f(x,y) \; \forall x \in \Omega$$
$$u(x,y) = 0 \; \forall x \in \partial\Omega$$
$$f(x,y) = x(8 - 2x^2 - 6y^2 + e^{3y}(1 - 3y(4+y) + x^2(-7 + 3y(4+3y)))$$

Here the solution is given by

$$u(x,y) = x(y^2 - 1)(x^2 - 1)(e^{3y} - 1)$$

Numerical results: goal functionals, effectivity index, meshes

We are interested in the functional evaluations:

$$J_0(u) := u(0.5, 0.5)$$

$$J_1(u) := \int_{\Omega_1} u(x,y) d(x,y)$$

$$J_2(u) := \int_{\Gamma_1} \nabla u(x,y).n \, d(x,y)$$

where $\Omega_1 = (-0.5, 0) \times (0.5, 1)$ and $\Gamma_1 = \{1\} \times (0, 1)$.

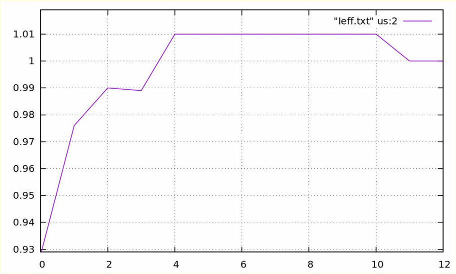

Figure: I_{eff} versus refinement levels.

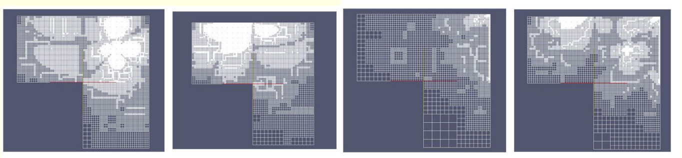

Figure: Mesh adaptation w.r.t. to J_1, J_2, J_3, J_c.

Numerical results: error plot

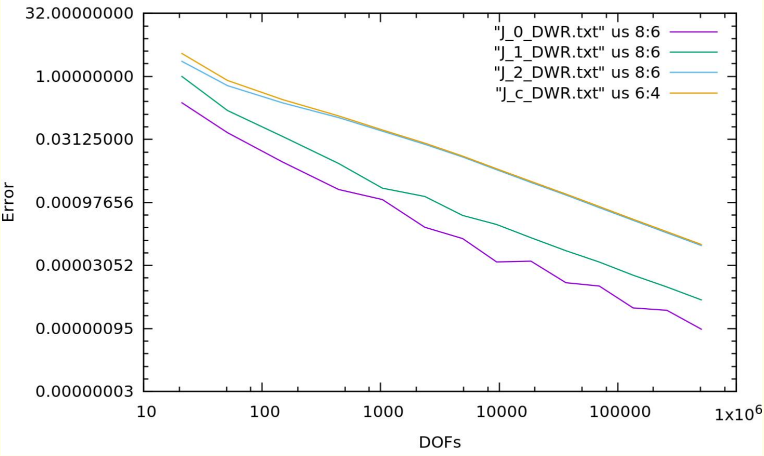

Figure: Relative error $\frac{|J_i(u)-J_i(u_h)|}{|J_i(u_h)|}$ versus DoFs.

Conclusions

Conclusions

- Modeling and robust algorithms (monolithic formulations!) for phase-field fractures;
- Computational analysis of the ε-h relationship and systematic development to measure goal functionals using a PU-DWR method;
- Extension of PU-DWR (currently for Poisson's problem) to multiple target functionals.

Key references of this talk

- T. Richter, T. Wick; Variational localizations of the dual weighted residual estimator; JCAM, 2015
- T. Wick; Goal functional evaluations for phase-field fracture using PU-based DWR mesh adaptivity; Comp. Mech. 2016

Conclusions

Conclusions

- Modeling and robust algorithms (monolithic formulations!) for phase-field fractures;
- Computational analysis of the ε-h relationship and systematic development to measure goal functionals using a PU-DWR method;
- Extension of PU-DWR (currently for Poisson's problem) to multiple target functionals.

Key references of this talk

- T. Richter, T. Wick; Variational localizations of the dual weighted residual estimator; JCAM, 2015
- T. Wick; Goal functional evaluations for phase-field fracture using PU-based DWR mesh adaptivity; Comp. Mech. 2016

The end for today - thanks!

The end for today - thanks!